IEEE INSTRUMENTATION & MEASUREMENT SOCIETY

Received 12 June 2022; revised 18 July 2022; accepted 28 July 2022. Date of publication 5 August 2022; date of current version 22 August 2022.
The review of this article was arranged by Associate Editor Sabrina Grassini.

Digital Object Identifier 10.1109/OJIM.2022.3196725

A MOSFET-Based Method for Measuring Peak Kilovoltage (kVp) in Diagnostic X-Ray Beams

FRANCISCO A. CAVALCANTI [1,2] AND LUIZ A. P. SANTOS [3,4] (Member, IEEE)

[1] Departamento de Energia Nuclear, Universidade Federal de Pernambuco, Recife 50740540, Brazil

[2] Departamento de Desempenho dos Sistemas, CHESF/Eletrobras Company, Recife 50761085, Brazil

[3] Nuclear Instrumentation Laboratory, CNEN/CRCN-NE, Recife 50740545, Brazil

[4] Technological Development Laboratory, Scients Company, Igarassu 53635015, Brazil

CORRESPONDING AUTHOR: L. A. P. SANTOS (e-mail: lasantos.scients@gmail.com)

This work was supported in part by CNPq Brazilian Agency under Grant 305017/2021-7, and in part by the Scients Company under Contract 200313.

ABSTRACT Peak kilovoltage (*kVp*) is an X-ray tube parameter that can influence the radiograph image quality and therefore, if the *kVp* is different from the nominal value, it can provide an unnecessary radiation dose to the patient if the examination has to be repeated. Therefore, some radiation protection institutions and health organizations (ICRP, IAEA) make recommendations to monitor *kVp* in medical diagnostic X-ray equipment in clinics and hospitals. There are some methods for measuring *kVp* in diagnostic X-ray beams, and the most common is the well-known two-sensor method, which uses two filters to attenuate the radiation beam, and it is based on the measurement of each identical sensor. The purpose of this article is to present a method for non-invasive measurement of *kVp* in medical diagnostic X-ray beams using the MOSFET device. Actually, MOSFET is well known as a detector for ionizing radiation dosimetry mainly in radiotherapy beams. Recently, MOSFET has also been used as dosimeter in diagnostic X-ray beams. In this work it will be shown a *kVp* measurement technique with MOSFET, which does not use the attenuation factor of the radiation filters, but instead takes advantage of the effect of the device package itself, known as the buildup cap effect. The results show that even with damage to the device exposed to radiation, MOSFET can be used as sensor for *kVp* measurement.

INDEX TERMS Instrumentation, MOSFET, peak kilovoltage, radiodiagnostic, X-ray.

I. INTRODUCTION

THE PEAK kilovoltage (*kVp*) of X-ray tubes used in clinics and hospitals is an important parameter to be monitored following recommendations made by some international organizations (e.g., IAEA, ICRP) [1], [2]. Actually, the *kVp* of an X-ray tube normally used in radiodiagnosis is a parameter that can influence the quality of the radiographic image and therefore can lead the patient to receive unnecessary radiation doses if the exam is repeated due to a blurred image, for example. This can occur mainly on older radiographic equipment, which is widely operational in Latin American and African countries, for instance. However, presenting an innovative technique may also have applications in other *kVp* measurement processes, even if it is not for clinical X-ray equipment.

Generally, the most common method for measuring *kVp* in X-ray tubes of clinical equipment is to use two identical radiation sensors, each with a radiation filter in front of the sensor [3], [4], [5], [6]. It is a non-invasive measurement technique with two sensors and radiation attenuation filters with different thicknesses, x_1 and x_2. As in radiodiagnosis the exposures are made with pulses of the order of tens or hundreds of milliseconds then, to avoid systematic errors [5], the X-ray pulse must be performed simultaneously on both sensors, and the result can be obtained by means of calculations as described in the literature [4], [5], [6], [7] (Fig. 1).

The method mentioned above is well known [4] and the *kVp* is basically estimated by (1), where S_1 and S_2 are the current signals (nA) from each sensor, x_1 and x_2 are the

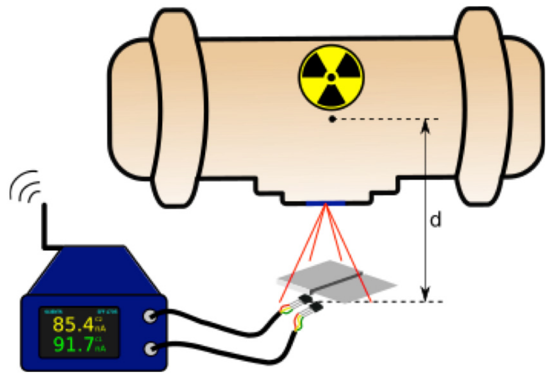

FIGURE 1. Illustration of a technique for measuring X-ray tube potential (*kVp*) in a non-invasive way with two identical radiation sensors, S_1 and S_2. Each sensor has a radiation attenuation filter with different thickness, x_1 and x_2. In this method S_1/S_2 rate can provide the *kVp* as shown in (1).

thickness of each radiation attenuation filter (mm), C_1 and C_2 correspond to the regression coefficients [3], [4], [5].

$$\mathrm{kVp} = \sqrt[\mathrm{C_2}]{\frac{\mathrm{C_1(x_2 - x_1)}}{\ln(\mathrm{S_1/S_2})}} \tag{1}$$

Actually, this method is based on determining the intensity I_x of a filtered spectrum such as that emitted by a typical X-ray tube [6], [7], [8], given by:

$$I_x = I_0 \int_0^{E_{max}} f(E) e^{-\mu(E)x} dE \tag{2}$$

where I_0 corresponds to the unfiltered X-ray beam, $E_{\max}$ is the maximum energy of the emitted photons, $f(E)$ is the distribution function of photons with energies between E and $E+dE$, $\mu(E)$ is the linear attenuation coefficient of the filter material for the energy E, and x is the filter thickness.

Silberstein [8] was the first to correlate I_x with the Laplace transform making:

$$f(E)dE = g(\mu)d\mu \tag{3}$$

to obtain:

$$I_x = I_0 \int_{\mu_0}^{\infty} g(\mu) e^{-\mu x} d\mu \tag{4}$$

By using the Laplace transform shifting property it results in:

$$\frac{I_x}{I_0} = e^{-\mu_0 x} \cdot \mathcal{L}\big[g(\mu - \mu_0)\big] = e^{-\mu_0 x} \cdot G(x) \tag{5}$$

where, μ_0 is the linear attenuation coefficient for $E_{\max}$, and $G(x)$ is a function that can be chosen appropriately to be able to reconstruct the filtered X-ray spectrum I_x [6], [7], [8], since $E_{\max}$ is correlated to kVp by:

$$kVp = q_e \cdot E_{max} \tag{6}$$

where q_e is the electron charge. However, Herrnsdorf [3] showed that, in fact, it is not necessary to reconstruct the spectrum to obtain the kVp. Instead, one can use the concept of effective attenuation coefficient, μ_{eft}, and the exponential attenuation equation:

$$I_x = I_0 \cdot e^{-\mu_{eft} x} \tag{7}$$

According to Lindström [9], μ_{eft} is correlated with both mean and effective energies of the X-ray spectrum and it can be assumed that:

$$\mu_{eft} = C_1 \cdot kVp^{-C_2} \tag{8}$$

Assuming that each filter x_1 and x_2 produces, respectively, I_{x1} and I_{x2} as a function of μ_{eft}, and also that S_1 and S_2 correspond to I_{x1} and I_{x2}, respectively, from (7) we have that:

$$\mu_{eft} = \frac{\ln(S_1/S_2)}{x_2 - x_1} \tag{9}$$

Combining (8) with (9) then results in (1). In this article it will be shown that if the sensors are two identical MOSFETs the technique presented based on (1) also works. However, the main purpose in this paper is to demonstrate experimentally that there is another way to measure the kVp of an X-ray tube without the need for two radiation filters. Before presenting the method, some information about the process of interaction of X-ray photons with the device is briefly discussed next.

Normally, the kVp value is chosen on the clinical X-ray equipment panel depending on the patient's weight. In medical diagnostic radiology these values can vary between 70 kV and 150 kV, depending on the type of organ to be radiographed and also on the type of equipment and the manufacturer. For the range 70-150 kV one can assume that the effective energy varies approximately between 50 keV and 100 keV where Compton effect is predominant [10], [11], [12], [13]. In fact, photon interactions occur with both the device package and the semiconductor chip and as both the package and the semiconductor material are of low atomic numbers then the probability of the Compton effect predominates for the energy range used in diagnostic X-ray beams [13]. Furthermore, there also are the Rayleigh and photoelectric effects, the latter occurring due to the photons scattered in the Compton effect, i.e., photons with lower energy. Actually, the package works as a build-up cap, which is a well-known effect [14]. Due to numerous interactions, an electron rain is generated in the MOSFET as shown in Fig. 2 [15]. Therefore, instead of beam attenuation, there is a build-up cap effect, which makes the signal to be measured stronger, i.e., the current in the semiconductor device, $i_d(t)$, increases. In the MOSFET, i_d signal is the drain current and can be measured in real-time during the X-ray pulse, shown next.

II. MATERIAL AND METHODS

A. MOSFET BIASING, SIGNAL MEASUREMENT AND AMMETER

The MOSFET biasing circuit is simple as shown in Fig. 3a. Analyzing a MOSFET switching curve (Fig. 3b), there is

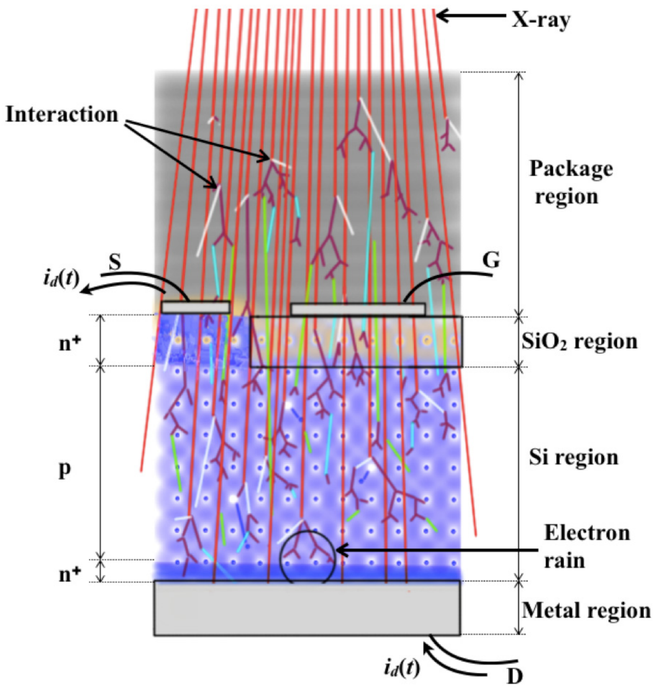

FIGURE 2. An illustration of numerous interactions generating the electron rain in a MOSFET where the device signal $i_d(t)$ is the drain current [15].

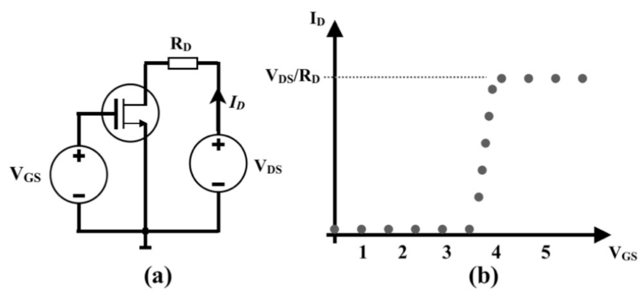

FIGURE 3. a) MOSFET bias; b) A MOSFET switching curve.

a cutoff region ($I_D \approx 2$ nA), a small range of V_{GS} where switching occurs, and a saturation region with the current $I_D = V_{DS}/R_D$. Therefore, $V_{GS} = 2.0$ V bias was chosen before the switching region for the following reasons: 1) X-ray irradiation on the MOSFET produces a shift in the curve to the left [16], [17]; 2) Switching region can generate signals with strong statistical fluctuation; 3) At the saturation ($I_D \approx 20$ μA) the sensitivity to the radiation is practically null, i.e., the drain current due to X-ray pulse can be much less than the saturation current.

During the X-ray pulse, the electron rain coming from package and chip itself generates a drain current called I_{DX}, to associate with the time interval in which the X-ray pulse occurs. That is, due to V_{DS} bias the signal $i_d(t) = I_{DX}$ is generated. Without X-ray beam the drain current is simply called I_D. To measure simultaneously two device samples an EFF1705 source-meter [18], Scients®, was used. Basically, it is a 0.1 nA resolution two-channel electronic system for measuring I_{DX} and I_D, and supply V_{DS} and V_{GS}.

TABLE 1. MOSFETs used in the Experiments and their characteristics.

MOSFET	Package	Thickness (mm)	I_D (A)	V_{DS} (V)	$R_{DS(on)}$ (Ω)
STD2HNK60Z-1	IPAK	1.46	2	600	4.8
STF2HNK60Z	TO220	1.60	2	600	4.8

TABLE 2. X-ray tube parameters for the clinical equipment used.

X-ray tube Parameter	Selectable values
Potential (kV)	52, 63, 77, 90, 102, 117, 125
Workload (mAs)	25, 50, 62.5, 80, 100, 125, 160, 200, 250, 320
Pulse time (ms)	25, 50, 100, 200, 400, 800, 1000, 1600, 2000

B. MOSFETS

Table 1 shows the device characteristics (mechanical and electrical). Information about the package thickness and its material (Ecopack) can be found in [19], [20].

Actually, the way found to perform an innovative method for measuring *kVp* with MOSFETs was to choose devices that are commercially available in two different types of packages. This means that both MOSFET devices have to be electrically identical (chip area, oxide thickness, drain-source resistance, capacitances, etc.) and can have different mechanical characteristics, specifically different packages, e.g., the thickness of the package between the device face and the chip face (Thickness in Table 1) [19], [20].

C. EXPERIMENTAL SETUP AND X-RAY PULSES

A clinical diagnostic X-ray equipment, Polymat Plus 30/50, Siemens®, was used to perform the experiments. For measurements using the most common method, Fig. 1 illustrates the experimental setup: two identical devices and each with a filter of different thicknesses: $x_1 = 1.0$ mm and $x_2 = 2.0$ mm. The distance between the X-ray source and the sensors was set to be d = 32.5 cm, for all experiments. The X-ray tube parameters can be chosen according to Table 2.

D. MEASUREMENT PROCEDURES

First, it was evaluated how is the signal behavior of a standard detector (10X5-6 ion chamber, Radical®) for the following X-ray tube parameters: 1600 ms exposure time for all experiments; 100 mAs and 200 mAs workloads; and varying the potential (*kVp*) from 52 kV up to 125 kV. The dose rate is proportional to the current signal produced by the sensor in each X-ray pulse [11], [15]. In each graph presented in the results each point corresponds to an average of 3 measurements. A total of 12 MOSFETs were used in all experiments as each measurement was performed in duplicate (two MOSFET samples).

The second procedure aimed to verify the repeatability in the I_{DX} measurement. The following X-ray tube parameters were taken: 1600 ms, 100 mAs, 102 kV. The experiments do not involve patients and for that reason after each X-ray pulse the clinical equipment had to be cooled down during 3 min (by technical recommendation), and therefore

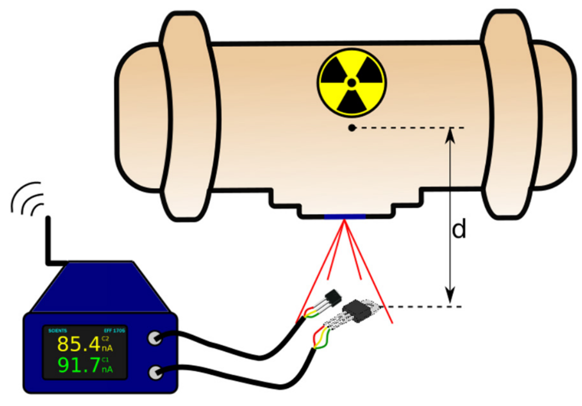

FIGURE 4. An illustration of two electrically identical MOSFETs with different packages irradiated without radiation attenuation filters.

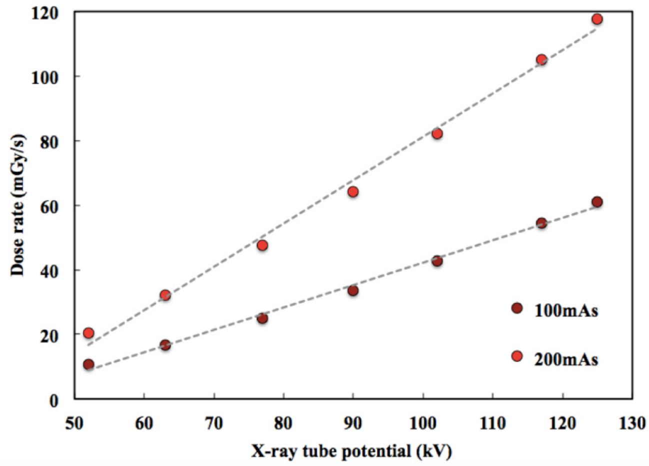

FIGURE 5. Response of a standard sensor to radiation pulses from clinical X-ray equipment as a function of *kVp* and parameterized by the workload: 100 and 200 mAs.

180 measurements of I_D were taken, so each point corresponds to an average of 180 readings. This timeout for the X-ray pulses also allows for some annealing to occur on the MOSFET. Actually, the value of I_D after each X-ray pulse corresponds practically to the ionization damage in the silicon oxide of the device, which generates a parasitic electric field as a function of the accumulated radiation dose. Therefore, it makes a shift in the MOSFET switching curve, which is a well-known effect [16], [17].

Knowing that there is repeatability on I_{DX} measurements, the third part of the experiments is correlated with the first part, which consists of comparing the MOSFET response with the response of the standard detector. A comparison of the results of two identical MOSFETs was also performed.

One of the methods in this paper is to verify if the MOSFET could be used in the usual two-sensor technique, i.e., it was placed radiation filters with different thicknesses on two electrically and mechanically identical devices. This procedure will lead us to conclude whether the MOSFET can be used by the known two-sensor method (see Fig. 1).

The fifth method performed in this work is basically the main one. Two electrically identical MOSFETs with different packages were exposed to the X-ray pulses without radiation attenuation filters as shown in Fig. 4. The X-ray tube parameters were: 1600 ms; 100 mAs; and varying the potential from 52 kV up to 125 kV.

Finally, our last experiment is to analyze how much scattering from the inherent radiation filter of the clinical equipment can reach the MOSFET under test. This can be done by varying the area of the radiation field in the X-ray equipment itself to perform I_{DX} measurements for each selected radiation field size. Scattered photons can make an additional contribution to measurements and thus produce a systematic error [14]. As the EFF1705 resolution is 0.1 nA, and in all the data the relative uncertainty were always less than 2%, a constant marker size was chosen to represent the error bar size, which is always smaller than the marker size.

III. RESULTS AND DISCUSSION

Firstly, Fig. 5 shows how the signal produced by the ion chamber behaves. It can be seen that the response of the standard sensor varies practically linearly with *kVp*. Regarding the workload, one can verify that by doubling the workload, the response also practically doubles. For example, the dose rate is 43 mGy/s for 102kV@100mAs, and about 82 mGy/s for 102kV@200mAs. As the X-ray pulse time is constant (1.6 s) then the X-ray tube current, I_{XRT}, corresponds to 62.5 mA and 125 mA, respectively. The current in the sensor is proportional to I_{XRT} [11], [15].

Fig. 6a shows results of I_{DX} measurements for a sequence of 30 X-ray pulses ($\approx$ 69 mGy each pulse), therefore the *x*-axis corresponds to $\approx$ 2.1 Gy accumulated radiation dose. It can be seen that there is repeatability in the measurements. In this set of I_{DX} measurements, the highest value of relative uncertainty was less than 1.5%. During the same sequence of X-ray pulses it was followed how I_D varied. The graph in Fig. 6b indicates that I_D increases about 200%, which corresponds to the ionization damage produced on the device during the irradiation.

Fig. 7 shows the MOSFET response to the X-ray pulses from the clinical equipment, and comparing with the standard sensor (Fig. 5) the similarity of behavior of both sensors can be noticed, it was expected [15]. The graph in Fig. 8 shows two identical MOSFET samples irradiated simultaneously to compare their responses. Basically, the difference in the curves consists in the sensitivity of each MOSFET, as in all types of sensor. In this case it is due to very small electrical and mechanical differences in their characteristics.

Fig. 9 demonstrates that, regardless of the workload, the MOSFET can be used as a sensor if the usual dual-sensor technique is preferred. However, as I_{DX} is higher for a workload of 200 mAs one can conclude that it is better to make the measurements by selecting a higher workload to minimize the relative uncertainties.

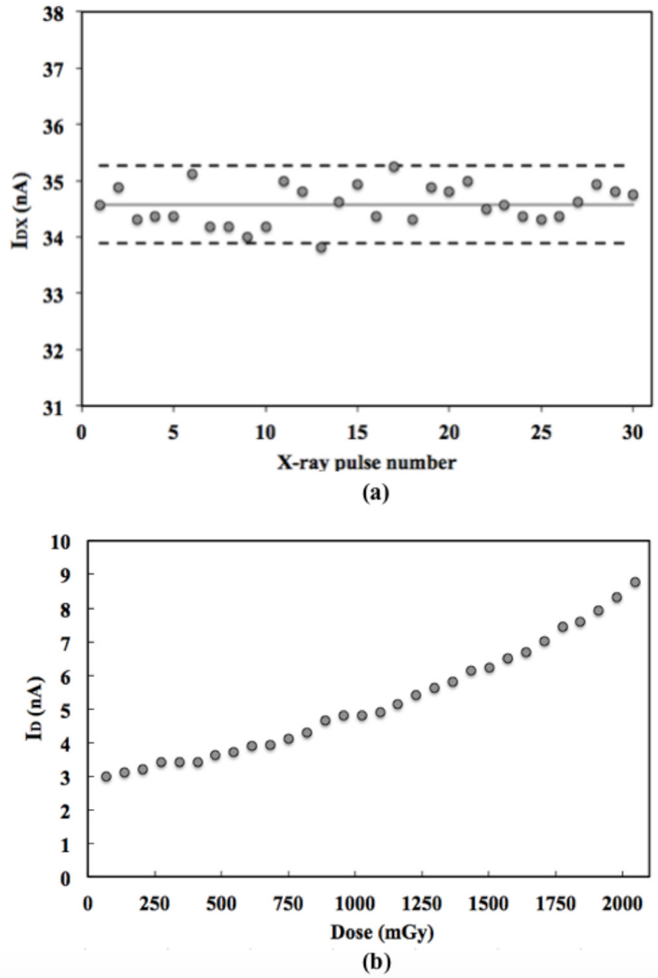

FIGURE 6. a) Repeatability of I_{DX} measurement in a sequence of 30 X-ray pulses with the average and ±2S limits; b) I_D as a function of the accumulated radiation dose during the 30 X-ray pulses.

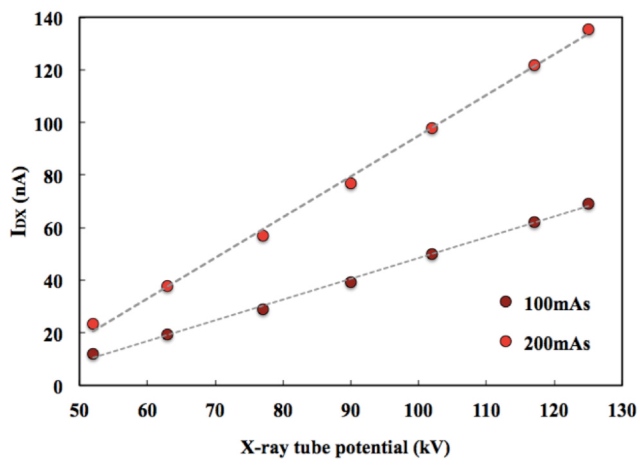

FIGURE 7. I_{DX} as a function of *kVp* parameterized by the workload: 100 and 200 mAs. The MOSFET response is similar to the standard sensor.

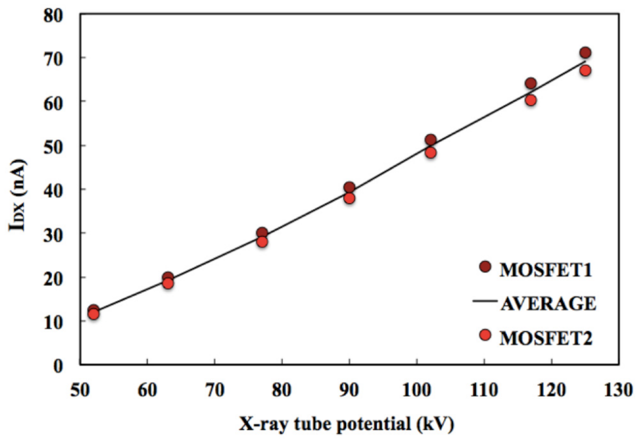

FIGURE 8. I_{DX} for two identical MOSFET samples simultaneously irradiated under an X-ray beam with parameters: 1600 ms; 100 mAs.

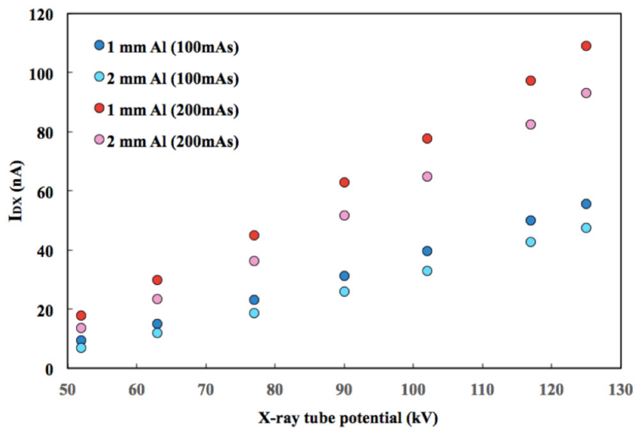

FIGURE 9. Responses to clinical X-ray pulses from two mechanically and electrically identical MOSFETs, S_1 and S_2, each with 1 and 2 mm thick radiation filters, respectively. The X-ray tube parameters were: 1600 ms: 100 and 200 mAs.

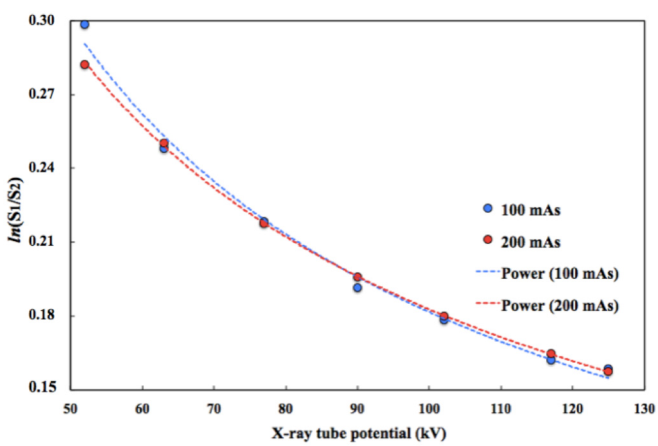

FIGURE 10. Regression fits for the MOSFETs in Fig. 9: The parameters of the X-ray tube were: 1600 ms; 100 mAs and 200 mAs workloads.

Fig. 10 presents two regression fits for the MOSFETs in Fig. 9. In both results, performed with 100 mAs and 200 mAs, there are similar regression coefficients as shown in Table 3, where C_1 and C_2 correspond to the regression of equation (10), i.e., it corresponds to the *x*-axis versus the *y*-axis (the inverse problem function).

TABLE 3. Values of regression coefficients of MOSFETs irradiated with aluminium filters (x_1 = 1 mm and x_2 = 2 mm) for two workloads: 100 mAs and 200 mAs.

Coefficients for equation (10)	100 mAs	200 mAs
C_1	4.976	4.002
C_2	0.719	0.670
R^2	0.9931	0.9998

TABLE 4. Percentage of scattered radiation by the inherent X-ray filtration of the clinical equipment.

Quantity	Values						
Field area (cm^2)	196	100	64	36	16	4	1
I_{DX} (nA)	44.3	43.8	43.3	42.9	42.9	41.2	40.2
Scattering eliminated (%)	-	1.0	2.1	3.0	3.1	6.9	9.2

$$kVp = \sqrt[C_2]{\frac{C_1}{\ln(S_1/S_2)}} \tag{10}$$

The main result of this work is shown in Fig. 11 where two electrically identical MOSFETs with different packages are irradiated without radiation attenuation filters in front of each device. In a simple comparison of Fig. 9 with Fig. 11 it is observed in the second one I_{DX} measurements are stronger without radiation filters even if a lower workload is selected. For example, the MOSFET produces $I_{DX} \approx 92$ nA for 100mAs@102kV without radiation filter, whereas with the 1 mm and 2 mm thick filter it produces $I_{DX} \approx 40$ nA and $I_{DX} \approx 33$ nA, respectively. Therefore, even performing the measurements with a workload of 100 mAs, a signal gain of more than 6dB is obtained in the experiment made without radiation filters.

For purposes of comparison, treating the data in Fig. 11 gives $C_1 = 3.286$, $C_2 = 0.543$ and $R^2 = 0.9915$, and therefore equation (1), which is proposed in the literature [3], [4], [5], [6] and [9], can be used without the need for radiation attenuation filters.

The last results of this paper are in Table 4 and Table 5. The first one presents the fraction of radiation scattered by the inherent radiation filtration of the clinical equipment. Note that the contribution of scattered photons reaches 9.2% (≈1-40.2/44.3) comparing the X-ray beam of 196 cm^2 with that of 1 cm^2, i.e., the scattering elimination is 9.2%. This leads us to conclude that the measurement of *kVp* must be performed with the collimated radiation beam, practically covering only the device area, to minimize the uncertainties and avoid a systematic error due to scattering. Table 5 shows two sets of relative uncertainties obtained in the experiment of Fig. 8. As the uncertainties (type B) of the X-ray generator and source-meter are 1% and 0.5%, respectively, it can be stated that the uncertainties u_1 and u_2, obtained from each device MOSFET1 and MOSFET2, respectively, are compatible with the expected value of type A uncertainties.

TABLE 5. Relative uncertainties (u_1 and u_2) as a function of *kVp* obtained in the measurements of Fig. 8 made with MOSFETs 1 and 2.

kVp	52	63	77	90	102	117	125
u_1 (%)	1.9	1.2	0.6	0.4	0.7	0.3	0.5
u_2 (%)	0.4	0.1	1.2	0.7	0.4	0.7	0.3

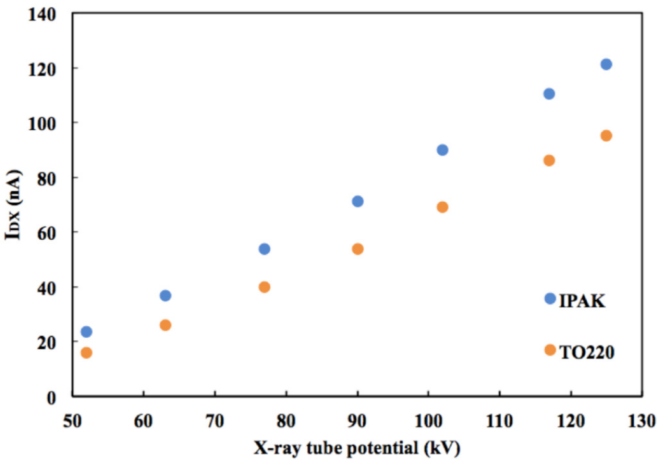

FIGURE 11. I_{DX} for two electrically identical MOSFET with different packages under X-ray pulses with the following parameters: 1600 ms and 100 mAs.

Finally, looking at the setup of the usual method in [4], it can be seen that there are radiation filters with their other required parts. Thus, from the point of view of kVp meter design, the proposed method presents less complexity, since there is a current signal gain and the technique becomes simpler. Also, from an industrial design point of view, it can be said that such an innovative technique implies an improvement in the economic factor of production.

IV. CONCLUSION

A non-invasive method based on electrically identical MOSFETs with different packages for measuring the potential (*kVp*) of diagnostic X-ray tube was presented. The usual method is based on the ratio of measurements from two identical sensors each with a radiation attenuation filter positioned in front of the device. The method proposed in this work does not use radiation filters, but instead uses the build-up cap effect, its own package, to obtain a signal gain and consequently achieve lower measurement uncertainties. The results showed that it is an innovative and valid technique. Also, the data obtained lead to the conclusion that it is more efficient to perform the measurements with a collimated X-ray beam.

ACKNOWLEDGMENT

The authors would like to thank Luiz C. Gonçalves Filho for his promptness in MOSFET irradiation procedures.

REFERENCES

[1] "Radiation protection of patients—RPOP." IAEA. Accessed: Mar. 27, 2020. [Online]. Available: https://www.iaea.org/resources/rpop/patients-and-public/x-rays

[2] *Annals of the ICRP: ICRP Publication 103*, ICRP, Ottawa, ON, Canada, 2007.
[3] L. Herrnsdorf, "Development and characterization of sensitive, energy-independent solid-state photon dosemeters with high spatial and temporal resolution—Applications in clinical radiology and radiation protection," Ph.D. dissertation, Dept. Transl. Med., Lund Univ., Malmö, Sweden, 2018.
[4] L. Büermann. "Non-invasive X-ray multimeters used in diagnosctics radiology." IDOS. 2019. Accessed: Jul. 16, 2021. [Online]. Available: https://www.iaea.org/events/idos2019/programme/day-4
[5] O. Kélpakotás, "Physical foundations of non-invasive X-ray tube voltage measurement," in *Book for Physicists*, 2nd ed. Budapest, Hungary: Semmelweis Univ., Feb. 2019. Accessed: Jun. 20, 2021. [Online]. Available: http://oftankonyv.reak.bme.hu/tiki-index.php?page=Physical+foundations+of+non-invasive+X-ray+tube+voltage+measurement&structure=Book+for+Physicistsage=Physical+foundations+of+non-invasive+X-ray+tube+voltage+measurement&structure=Book+for+Physicists
[6] V. Delgado, "Determination of x-ray spectra from attenuation data by imposing a priori positiveness and bounded support: Theory and experimental validation," *Med. Phys.*, vol. 34, pp. 994–1006, Mar. 2007.
[7] J. R. Greening, "The determination of X-ray wavelength distributions from absorption data," *Proc. Phys. Soc.*, vol. A63, no. 11, pp. 1227–1234, May 1950.
[8] L. Silberstein, "Determination of the spectral composition of X-ray radiation from filtration data," *J. Opt. Soc. America*, vol. 22, no. 5, pp. 265–280, 1932.
[9] J. Lindström, *The Non-Invasive X-Ray Multimeter—Principles, Advantages, Drawbacks and Uncertainties*, 4th ed. Stockolm, Sweden: Karolinska Universitetjukhuset, 2016, pp. 3–32.
[10] T. Haba *et al.*, "Pin-photodiode array for the measurement of fan-beam energy and air kerma distribution of X-ray CT scanners," *Physica Medica*, vol. 32, pp. 905–913, Jul. 2016.
[11] *Diagnostic Radiology Physics: A Handbook for Teachers and Students*, IAEA, Vienna, Austria, 2014.
[12] D. McLean, "X-ray spectra and beam qualities," in *Proc. Joint ICTP-IAEA Adv. School Dosimetry Diagn. Radiol.*, Trieste, Italy, May 2009, pp. 11–15.
[13] A. Lechner, "CAS-CERN accelerator school: Beam injection, extraction and transfer," CERN Accelerator School, Erice, Italy, CERN Yellow Rep. CERN-2018-008-SP, 2018.
[14] E. Turner, *Atoms, Radiation, and Radiation Protection*, 3rd ed., Willey-VCH Verlag GmbH Co., Weinheim, Germany, 2007.
[15] L. A. P. Santos, "An overview on bipolar junction transistor as a sensor for X-ray beams used in medical diagnosis," *Sensors*, vol. 22, no. 5, p. 1923, 2022.
[16] L. C. G. Filho, D. S. Monte, F. R. Barros, and L. A. P. Santos, "Radiation dose response of n-channel MOSFET submitted to filtered X-ray photon beam," *IEEE Trans. Nucl. Sci.*, vol. 65, no. 9, pp. 2607–2610, Sep. 2018.
[17] D. S. Monte and L. A. P. Santos, "A method for measuring ionizing radiation dose by analyzing hybrid-π parameters of transistors," in *Proc. IEEE Int. Instrum. Meas. Technol. Conf. (I2MTC)*, 2020, pp. 1–6, doi: 10.1109/I2MTC43012.2020.9129059.
[18] "EFF1705 source-meter." Accessed: May 15, 2022. [Online] Available: http://www.scients.com.br/produto/
[19] "N-channel 600 V, 3.5 Ohm typ., 2 A SuperMESH power MOSFET in a TO-220FP package," STF2HNK60Z MOSFET Datasheet, STMicroelectronics, Geneva, Switzerland, 2021. [Online] Available: https://www.st.com/en/power-transistors/stf2hnk60z.html
[20] "N-channel 600 V, 3.5 Ohm typ., 2 A SuperMESH power MOSFET in an IPAK package," STD2HNK60Z-1 MOSFET Datasheet, STMicroelectronics, Geneva, Switzerland, 2021. [Online]. Available: https://www.st.com/en/power-transistors/std2hnk60z-1.html

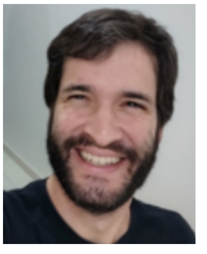

FRANCISCO A. CAVALCANTI was born in Recife, Brazil, in 1982. He received the B.S. degree in electronics engineering in 2006, and the M.S. and Ph.D. degrees in nuclear technology from the Federal University of Pernambuco, Recife, in 2014 and 2022, respectively. From 2007 to 2009, he was an Instrumentation Engineer with the Petrobras company. From 2010 to 2011 he was teaching with the Instituto Federal de Pernanbuco. Since 2011, he has been an Electronics Engineer with CHESF/Eletrobras Company.

LUIZ A. P. SANTOS (Member, IEEE) was born in Recife, Brazil, in 1963. He received the B.S. degree in electronics engineering and the M.S. degree in nuclear technology from the Federal University of Pernambuco, Recife, in 1987 and 1992, respectively, and the Ph.D. degree in geophysics from University Joseph Fourier, Grenoble, France, in 1997. Since 1998, he has been a Researcher with Nuclear Instrumentation Laboratory, CRCN-NE/CNEN, and since 2011, he also has been the part-time Head of the Technological Development Laboratory, Scients Company. He is the author of 25 articles and 13 inventions and holds four patents. His research interests include instrumentation, sensors, semiconductors, radiation, geophysics, environment, and applied physics.